Volume 1, Number 1 (December 2005) p. 75-90 ISSN 1809-5046
Revista IBRACON de Materiais
IBRACON Materials Journal

Carbonation Behavior in Reinforced Concrete Beams Under Stress Regime

O Comportamento da Carbonatação em Viga de Concreto Armado sob Regime de Tensão

V. M. Silva [a]
vms@sc.usp.br
J. B. L. LIBORIO [b]
liborioj@sc.usp.br
M. de CASTRO [c]
mcastro@icmc.usp.br

Abstract

This work reports results obtained by studying the behavior of reinforced concrete beams under a tension-testing regime, in which the beams were exposed to an environment with high CO_2 concentration. Beam molding followed by humid cure required 7 days and the subsequent application of a two-point load with the lowest possible frame dimensions in a controlled atmosphere 80% of which was concentrated CO_2; relative humidity was 6065%. Carbonation depth results, cracks, as well as the cover's effectiveness in reinforcement protection, were analyzed with respect to beam serviceability.

Keywords: beam; carbonation; concrete; crack; durability.

RESUMO

Este trabalho refere-se à simulação do comportamento de elementos de estruturas (vigas) de concreto armado sob regime de tensão, na condição fissurada e exposta a um ambiente com elevada concentração de dióxido de carbono. Realiza-se a moldagem do elemento estrutural seguindo-se sua cura úmida, por 7 dias, e posterior solicitação nos terços, na máxima condição de sub-armação, e em seguida a viga é submetida a atmosfera controlada com concentração de 80% de CO_2 e U.R. = 60 ± 5%. São discutidos os resultados da profundidade de carbonatação, fissuras e a efetividade do cobrimento na proteção da armadura, na condição de serviço.

Palavras-chave: viga, fissura, carbonatação, durabilidade, concreto, cobrimento.

[a] Ph.D. Candidate in Department of Structural Engineering and Researcher of the Cement Based Advanced Materials Laboratory at the Engineering School of São Carlos, São Paulo University

[b] Professor, Coordinator of the Cement Based Advanced Materials Laboratory - Department of Structural Engineering at the Engineering School of São Carlos, São Paulo University - Av. Trabalhador São-carlense, 400, centro, São Carlos/SP – CEP:13566-590

[c] Assistant Professor, Computer Science and Statistics Department, São Paulo University at São Carlos

1 Introduction

At present, the most pressing problem relating to the durability of reinforced concrete structures is reinforcement corrosion. When hydrated, portland cement produces portlandite, $Ca(OH)_2$, resulting in alkalinity with pH around 12.5 in the concrete. This alkalinity chemically protects the steel bars through the formation of an oxide-based passive protection film (1).

However, concrete carbonation reduces the pH to approximately 8.3, (1, 2), which destroys the oxide film, leaving the steel exposed. In itself, this does not automatically produce corrosion, which only begins when the relative humidity exceeds 80%.

Several mathematical models have been developed to relate carbonation depth with time (3, 4). One of the models most frequently used in technical work is $x = k \cdot \sqrt{t}$ where x represents carbonation depth in mm; t, the time of exposition in years; and k, the carbonation coefficient.

The carbonation effect in reinforced concrete beams under maximum strain with a minimally dimensioned frame is verified in this study (5). To guarantee reinforcement protection and, consequently, the durability of a structure, cracking must be avoided (5, 6). Code 6118/2003 established by the Brazilian Association for Technical Code Determination (7) classes cracking in reinforced concrete according to the type of environmental aggression; by the standard adopted, such cracking may vary from 0.2 mm to 0.4 mm. This code also specifies the nominal cover and water/cement relationship to be adopted for concrete in accordance with the degree of aggression in the environmental type to which the structure will be exposed.

1.1 Experimental details

The experiment required a 90 cm x 60 cm x 488 cm accelerated carbonation chamber, which was built out of steel plates and reinforced with metal supports.

This chamber maintained a 65% ± 5% relative humidity, had an 80% carbon dioxide concentration, a 50 mmH2O internal pressure, and was kept at ambient temperature.

Carbonation depth determination was obtained using a phenolphthalein solution to indicate pH. This solution, which turns lilac when concrete is alkaline and does not alter the color of carbonated concrete, was prepared using 1% phenolphthalein, 70% ethyl alcohol, and 29% distilled water.

Reinforced concrete beams, with rectangular sections 15 cm x 30 cm and 300 cm long, were submitted to flexure. Specimens 100 mm in diameter and 200 mm in height were submitted to axial compression, tensile strength, accelerated carbonation, and Young's modulus testing.

An analysis of ideal aggregate composition was also carried out, following (8). Data for concrete used in molding beams 1 and 2 are shown in Table 1.

The beams were tested by applying a two-point loading to a steel cable, using a hydraulic jack. The loads consisted of two concentrated forces of the same intensity. The test was static and used bi-supported beams (Fig. 1).

Figure 1 – Loading application and instrumentation.

The reinforced concrete beam was cured for 7 days after being molded. External instrumentation of the beam was carried out, and external prestress loading was applied. Readings of crack opening were done with graduated magnifying glass having 0.01 mm accuracy. The samples were then put in a chamber for humidity stabilization, which was reached in 21 days, following which carbon dioxide was injected for a period of 28 days. Loading was maintained during the entire period in which the beam stayed in the chamber.

To measure loading throughout the test period, a load cell positioned at one end of the prestress cable registered the prestress loss of tensile strength during compression and throughout the test.

Strain gauges were positioned on both longitudinal and transversal steel bars, and on the concrete to determine strains. A uniaxial strain gauge was used on each longitudinal steel bar. Two strain gauges were used on the transversal steel bars and positioned at mid-height of the stirrup. Three strain gauges were used in the concrete, and placed in the middle of the beam's span in the compressed area.

Table 1 – Mix proportion of concretes used in the molding of beams 1 and 2.

Cement	Mix 1:m	Mix 1:a:p	a / ag.	SP (%)	Consistency (mm)	C (kg / m^3)
CP II E-32	1:5.0	1:2.06:2.94	0.47	0	100	379.3
	1:4.64*	1:1.88:2.76	0.40	0.4	100	414

** Addition of 10% silica fume in a volumetric substitution of cement*

Where: *C = cement consumption and SP = superplasticizer.*

Periodic readings of active loading value in the beam were performed using a selector box connected to a control. With this equipment, readings from strain gauges attached to the concrete and the longitudinal and transversal steel bars during the entire testing period were also obtained.

During prestress, the dial gauges were positioned on the supports and in the middle of the span (Fig. 1). During the period in which the beam remained in the carbonation chamber, displacement in the middle of the span was monitored through the dial gauges.

Readings of opening cracks were carried out after removing the beam from the carbonation chamber and, only later, prestress ceased. The beam was dissected, to verify carbonation depth by extracting samples with a diamond-faced drill 7.0 cm in internal diameter. Also carbonation was determined in concrete specimens cured for 7 days in a humid chamber and deposited together with the beam in the carbonation chamber.

Carbonated depths were measured along the beam, in both the cracked and uncracked area, using a pachimeter with 0.05 mm precision. Carbonated depth average resulted from the totality of results of the six readings carried out in each specimen.

2 Results and Discussion

Figs. 2, 3, 4, and 5 present, respectively, the results obtained for axial compression strength, tensile strength, and elasticity as determined by Young's modulus in specimens of the concrete used in molding beams 1 and 2.

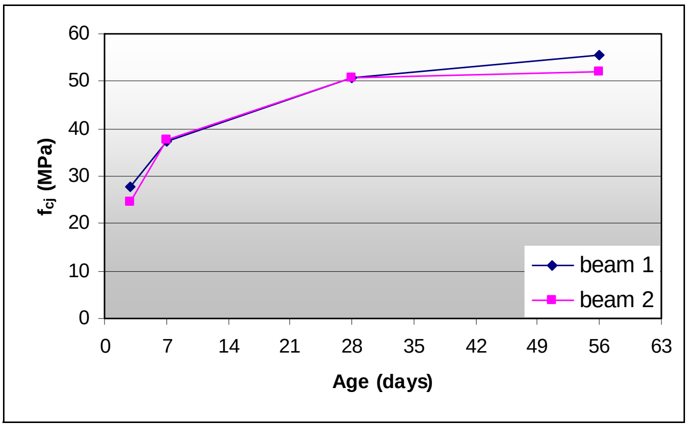

Figure 2 – Axial compressive strength of concrete specimens from beams 1 and 2.

The results of Young's modulus for specimens submitted to humid cure are not comparable to those of the ones that were treated in the carbonation chamber because, as they were exposed to different atmospheric conditions, they presented different internal humidity. In the tests to characterize the steel bars, samples having diameters of 5.0 mm, 6.3 mm, and 12.5 mm were used; Young's modulus and yield strength values appear in Table 2.

Table 2 – Young's modulus and yield strength values of steel bars CA-50.

Diameter	Young's modulus E (GPa)	Yield strength f_{yd} (MPa)
12.5	202.0	566
6.3	209.5	551
5.0	207.3	555

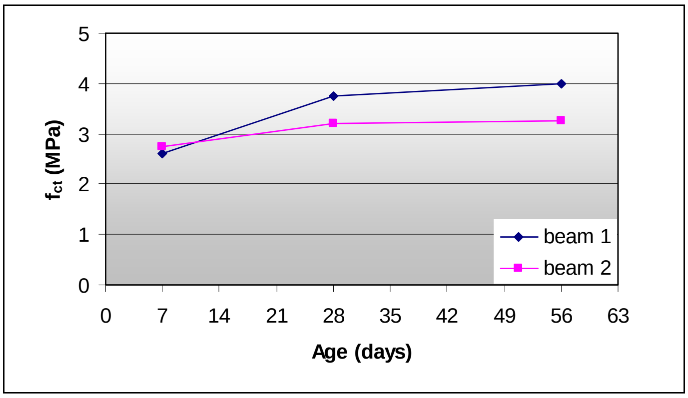

Figure 3 – Tensile strength of concrete specimens from beams 1 and 2.

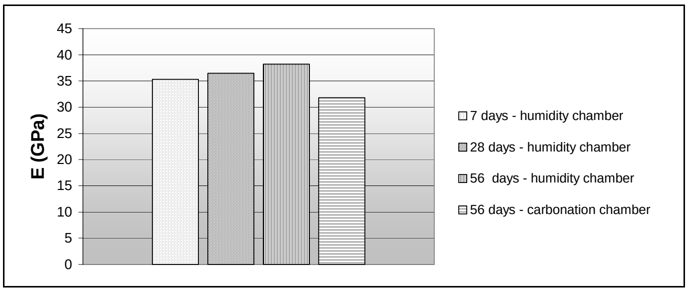

Figure 4 – Young's modulus results from concrete specimens from beam 1.

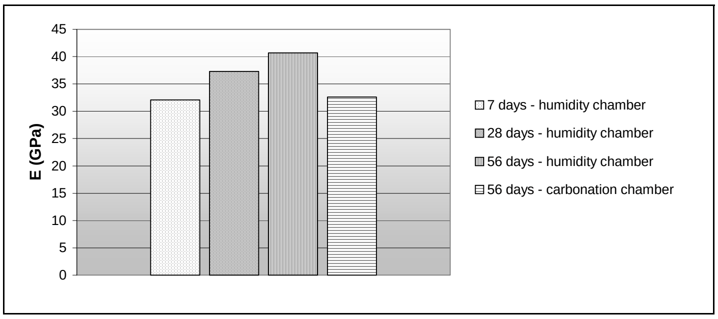

Figure 5 - Young's modulus results from concrete samples from beam 2.

2.1 Carbonation of beams 1 and 2

The graphs in Figs. 6 and 8 indicate carbonation depths in concrete specimens 100 mm in diameter and 200 mm in height, following the period spent in the carbonation chamber. The graphs in figs. 8 and 11 show carbonation depths of samples 70 mm in diameter and 150 mm in height, extracted from carbonated beams 1 and 2. The carbonation depth of the samples is not the same as that obtained in those extracted from the beams, but the averages of these sets of values do not differ significantly. Figs. 7 and 10 illustrate the position of the specimens extracted from beams 1 and 2.

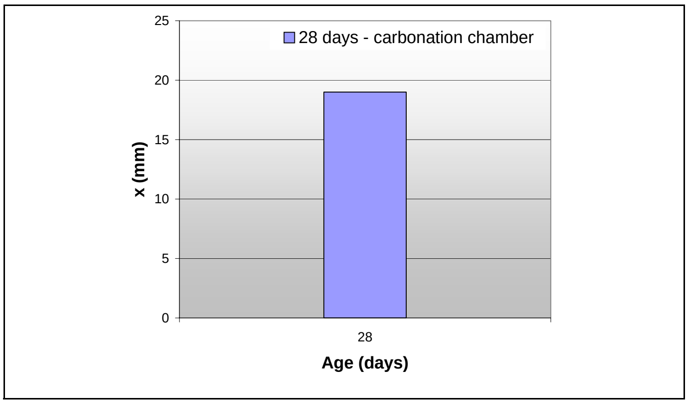

Figure 6 – Carbonation depth of concrete specimens cured for 7 days in humidity chamber, 21 days for humidity stabilization, and 28 days in carbonation chamber (beam 1).

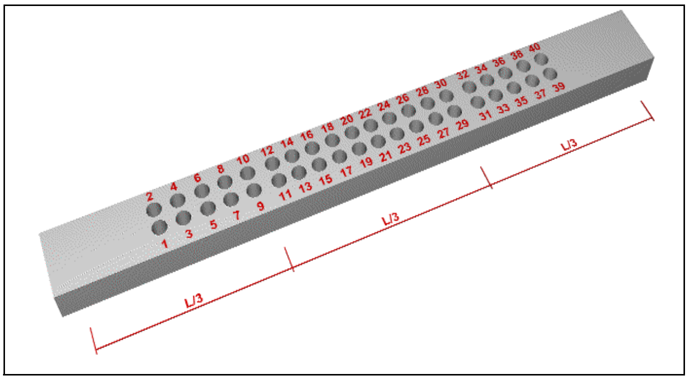

Figure 7 – Position of samples extracted from beam 1.

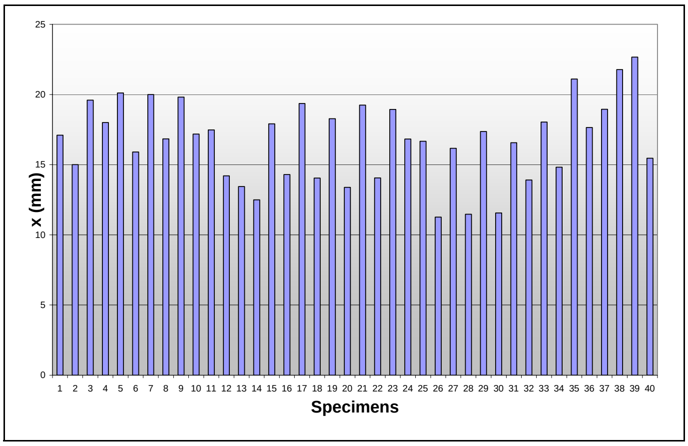

Figure 8 – Carbonation depth of the samples extracted from beam 1.

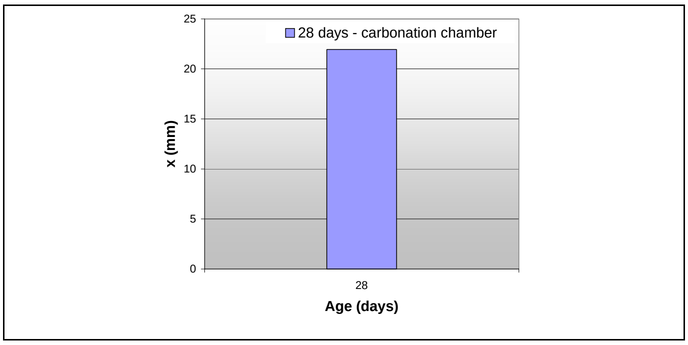

Figure 9 - Carbonation depth of concrete specimens cured for 7 days in humidity chamber with 21 days for humidity stabilization, and 28 days in carbonation chamber (beam 2).

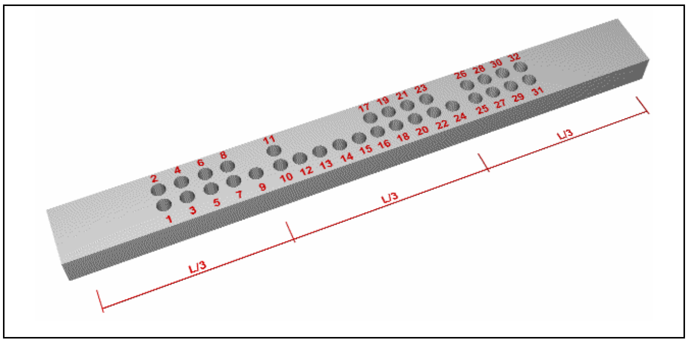

Figure 10 – Position of samples extracted from beam 2.

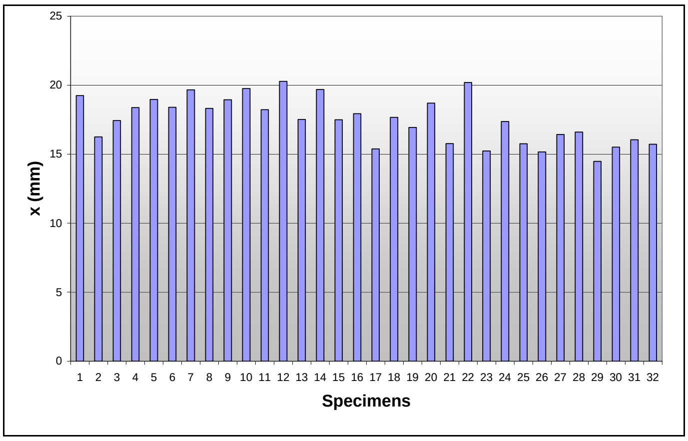

Figure 11 – Carbonation depth of samples extracted from beam 2.

Figs. 8 and 11 show that the results in carbonation depths are not uniform throughout the two beams. However, a tendency to behave differently was observed when comparing the upper and lower areas of the beam samples and also with respect to each of the thirds. In addition, an area found among the thirds presents a constant flexure moment, while in two others it varies.

2.2 Beam loading

For purposes of comparison, two procedures (P1 and P2) for calculating displacement and strain were tested. In P1, the inertia of a gross concrete section (Ig) was considered; P2 considered the inertia of the homogenized section.

2.2.1 Beam 1

The inertia value of the gross section was less than that of the homogenized section. Therefore, the cracking moment of P1 is smaller than that obtained for P2.

The graph in Fig. 12 presents the results for vertical load x displacement in the middle of the beam span. At the same moment in which the vertical load reached approximately 20.0 kN, the direction in the graph changed; this behavior coincided with the appearance of the first crack in the concrete. After loading, wedging was carried out and the beam was submitted to the carbonation test. Vertical load reduction due to prestress loss during wedging is clear in the graph in Fig. 12. Soon afterwards, stabilization was indicated by the vertical load readings, which refer to humidity stabilization (21 days) and that of accelerated carbonation (28 days). In P1 and P2, the displacements are greater than in the experimental case; P2 is the one which most resembles the control.

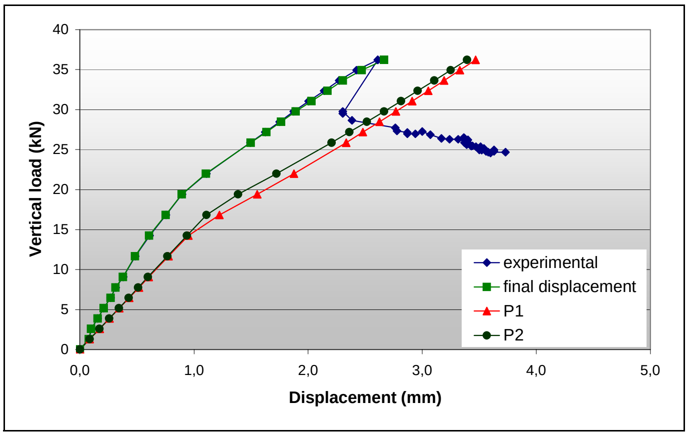

Figure 12 - Vertical load x displacement in the middle of the beam span.

The value obtained in the experiment corresponds to the average of the two dial gauges positioned in the middle of the beam span, whereas the final displacement is the average value of the same dial gauges minus the average of the dial gauge readings placed at each end of the same beam.

The vertical load x concrete strain results, referring to the three strain gauges attached to the middle span of beam in the compressed area are presented in the graph shown in Fig. 13. The same behavior as previously seen repeats itself: change of stage, prestress loss due to wedging, theoretical strains larger than those produced by the experiment, and stabilization of the vertical load readings throughout the period.

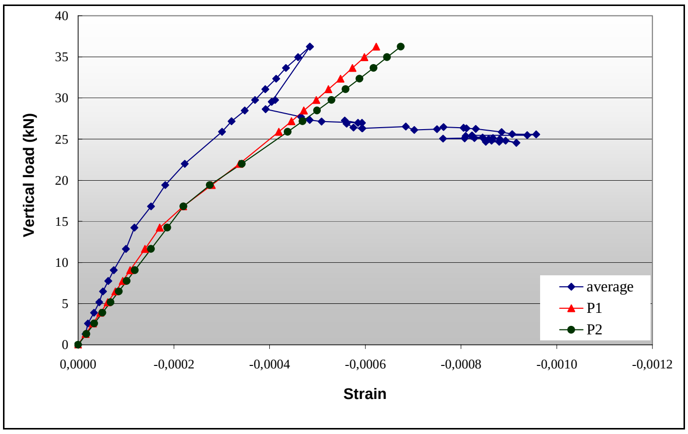

Figure 13 – Vertical load x strain of concrete in the middle of the beam span.

In Figs. 14 and 15 the graphs show, respectively, the results of vertical load x strain in the lower and upper layer of positive reinforcement. After wedging, a decrease in vertical load appears and afterwards strain decrease in the steel bars occurs. In Stage I, the theoretical strain exceeds that obtained experimentally, while in Stage II, the values are smaller to the experimental ones. It is worth mentioning that P1 favors safety.

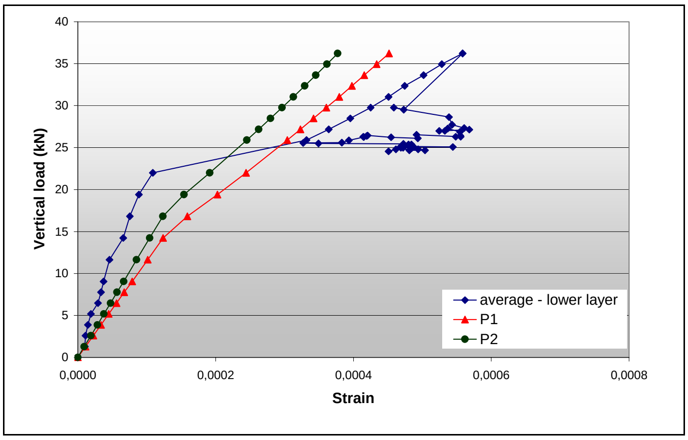

Figure 14 – Vertical load x average strain of three steel bars positioned in lower layer.

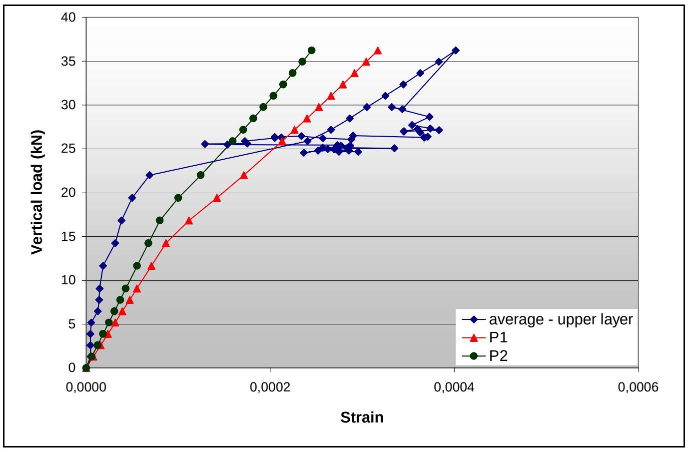

Figure 15 – Vertical load x average strain of two steel bars positioned in upper layer.

2.2.2 *Beam 2*

For beam 2, the same methodology used to analyze beam 1 was applied. In Figs. 16 and 17, the graphs show that the behavior of both displacement and concrete strain is similar to that observed for beam 1 in the graphs appearing in figs. 12 and 13.

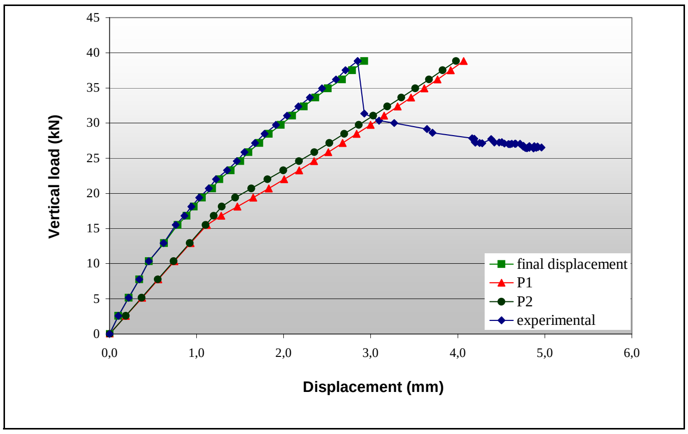

Figure 16 – Vertical load x strain of concrete in the middle of the beam span.

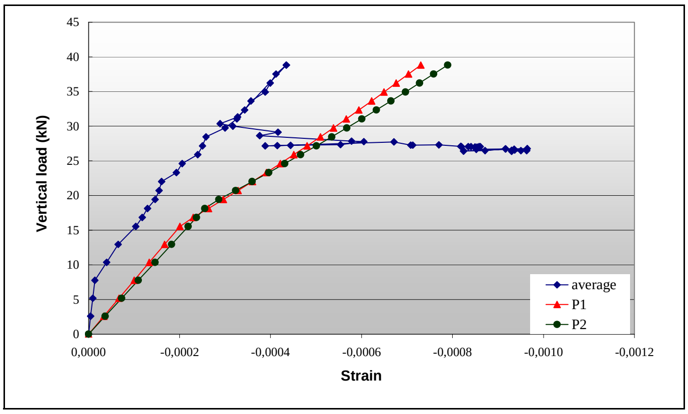

Figure 17 – Vertical load x strain of concrete in the middle of the beam span.

The graphs in figs. 18 and 19 demonstrate the results of vertical load x strain in the lower and upper layer of positive reinforcement. The theoretical results resembled the experimental ones and, again, P1 favors safety.

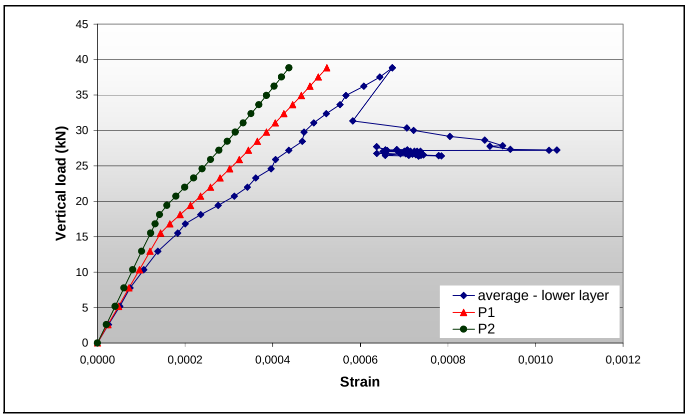

Figure 18 – Vertical load x average strain of three steel bars positioned in the lower layer.

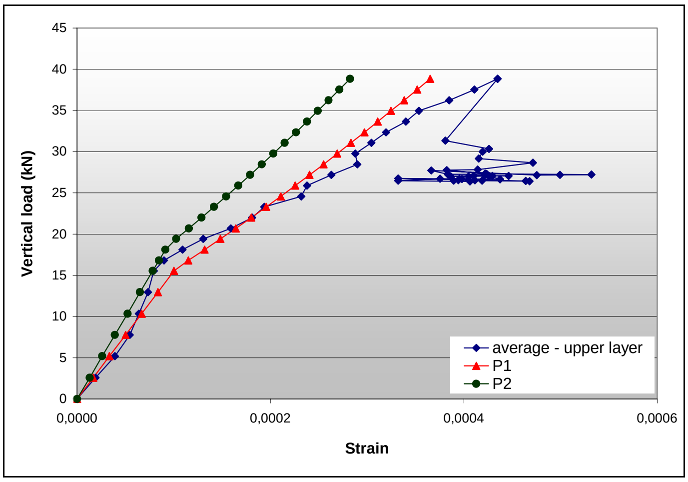

Figure 19 – Vertical load x average strain of two steel bars positioned in upper layer.

2.3 Cracks

The readings of crack openings in beams 1 and 2 showed a minimum 0.02 mm value and a 0.16 mm maximum for beam 1; for beam 2, the minimum was 0.02 mm and the maximum, 0.14 mm. The tests involving accelerated carbonation were performed on samples extracted from beams, and at the height from which they were extracted the carbonation surface had diffused along the cracks, as shown in Fig. 20. It is important to emphasize that the samples extracted were located directly above the steel bars, therefore carbonation was found in the same position as that of the reinforcement. Thus, reinforcement at that point was unprotected even though high performance concrete was used. Consequently, additional protection is required when employing these same materials under similar circumstances.

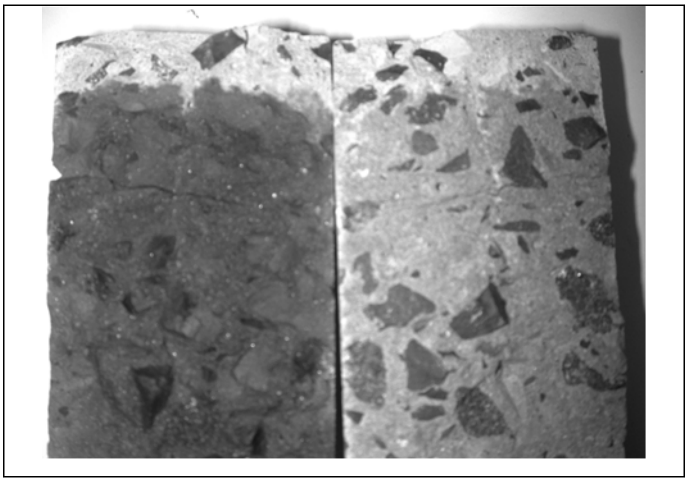

Figure 20 – Specimens extracted from reinforced concrete beam showing carbonation behavior along the crack.

2.4 Statistical analysis

For statistical analysis, a nonparametric test of Mann-Whitney was used, as well as variance analysis (ANOVA) with 5% level significance.

In agreement with the Mann-Whitney, there was no significant difference between samples from beams 1 and 2 with respect to the following: axial compressive strength at 3, 7, 28, and 56 days ($p = 0.25$; $p = 1.0$; $p = 0.70$; $p = 0.40$, respectively); tensile strength at 7, 28, and 56 days ($p = 0.0765$; $p = 0.20$; $p = 0.20$, respectively); and Young's modulus of elasticity at 7, 28, and 56 days ($p = 0.40$; $p = 0.70$; $p = 0.0765$, respectively). It should be emphasized that all of these values refer to samples submitted to humid curing.

The Mann-Whitney test revealed no significant difference in carbonation depth at 56 days ($p = 0.70$) between samples from the two beams.

The statistical analysis demonstrated that: the difference between the two beams was not significant ($p = 0.274$), the difference among the thirds was significant ($p = 0.00185$), and the difference in relation to the position from which the specimens were extracted from the beam was significant ($p < 0.0005$).

3 Conclusions

Serviceable beams were shown to present cracks that allow surface diffusion of carbonation in areas above the beam cover, thus damaging the protective character of the reinforcement. Therefore, the concrete cover is only one of the possible parameters to consider in preventing the action of carbon dioxide.

Carbonation depth was not uniform along the surface of the stressed structural member. The statistical analysis showed surface diffusion of carbonation in the thirds, a behavior that depends on loading distribution.

The present paper shows that a difference existed in carbonation depth in relation to the position from which the samples were extracted from the beams. The carbonation depth tended to be greater in the tensile area and lesser in the compressed area, which was due

to diffusion's being facilitated in the first area but hindered in the second.

The statistical analysis performed showed that beams 1 and 2 presented no significant differences, revealing good efficiency in the use of silica fume.

4 Acknowledgements

The authors are grateful to FAPESP for financial support.

5 References

[1] COMITE EURO INTERNATIONAL du BETON/CEB, Durability of concrete structure. state of art report, Bulletin D'information, n. 148, Munich, 1982.

[2] COMITE EURO INTERNATIONAL du BETON/CEB, Durability of concrete structure: Final report of CEB-RILEM International. Bulletin D'information, n. 152, Copenhagen, 1983.

[3] SILVA, V.M., Contribuição ao estudo da carbonatação em concretos e argamassas executados com e sem adição de sílica ativa. Interunidade EESC-IFSC-IQSC, Universidade de São Paulo, São Carlos, Dissertação, 2002.

[4] RICHARDSON, M.G., Carbonation of reinforced concrete: Its causes and management. New York: CITIS Ltd, Publishers, 1988.

[5] SILVA, V.M. Análise experimental de vigas de concreto armado, submetidas à ação da carbonatação, sob regime de tensão. Doutorado em andamento em Engenharia de Estruturas. Universidade de São Paulo, São Carlos/SP. Processo FAPESP no 02/06888-9.

[6] CASTEL, A.; FRANCOIS, R.; ARLIGUIE, G., Effect of loading on carbonation penetration in reinforced concrete elements. Cement and Concrete Research, v. 29, p. 561-565, 1999.

[7] Associação brasileira de normas técnicas. NBR 6118: Projeto de estruturas de concreto - procedimento, Rio de Janeiro, 2003.

[8] HELENE, P.R.L.; TERZIAN, P., Manual de dosagem e controle do concreto. Brasília - DF: Pini, 1992.